

# QCD phase diagram for small densities from simulations at imaginary $\mu$

P. de Forcrand<sup>a</sup> and O. Philipsen<sup>b</sup> \*

<sup>a</sup>ETH, CH-8093 Zürich, Switzerland and CERN Theory Division, CH-1211 Geneva 23, Switzerland

<sup>b</sup>Center for Theoretical Physics, MIT, Cambridge, MA 02139-4307, USA

We present results on the QCD phase diagram for small densities without reweighting. Our simulations are performed with an imaginary chemical potential  $\mu_I$  for which the fermion determinant is positive. On an  $8^3 \times 4$  lattice with 2 flavors of staggered quarks, we map out the pseudo-critical temperature  $T_c(\mu_I)$ . For  $\mu_I/T \leq \pi/3$ , this is an analytic function whose Taylor expansion converges rapidly, with truncation errors smaller than statistical ones. The result is analytically continued to give the location of the pseudo-critical line for real  $\mu_B \lesssim 500$  MeV.

## 1. INTRODUCTION

In view of heavy ion collision experiments a pressing task for lattice QCD is to map out the deconfinement transition in the  $(\mu, T)$ -plane. The complexity of the fermion determinant at finite baryon density renders standard Monte Carlo techniques impossible [1]. One way of circumventing this ‘sign problem’ are multi-dimensional reweighting techniques, and a phase diagram has been presented last year [2]. Reweighting generally breaks down for large volumes and/or densities, and one difficulty of the approach is to know when that happens. In [3] both reweighting factor and observables were expanded in a Taylor series in  $\mu/T$ , and the first coefficients were measured [3]. This method allows to simulate larger volumes, but a priori nothing is known about the error introduced by truncating the series.

Here we present an alternative method avoiding reweighting altogether. We simulate at imaginary  $\mu$  for which there is no sign problem and arbitrarily large volumes are feasible. Observables are fitted by truncated Taylor series in  $\mu/T$ , keeping full control over the associated systematic error. The series may then be continued to real  $\mu$ , provided the observable is analytic [4]. This strategy has been successfully tested for screening masses [5], here we extend it to the critical line itself. A detailed account of this work is given in [6].

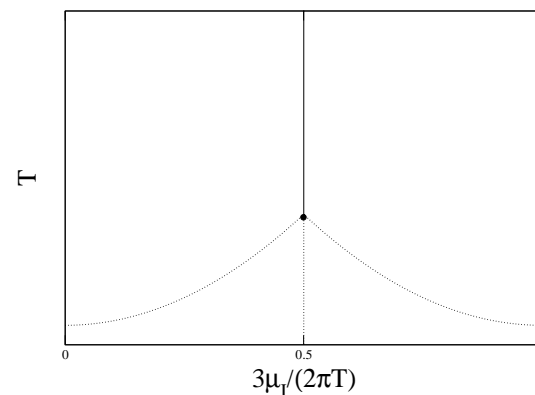


Figure 1. Phase diagram in the  $(\mu_I, T)$ -plane. The vertical line marks a  $Z(3)$  transition crossing the deconfinement transition. For  $T > T_c$  the former is of first order.

## 2. QCD AT IMAGINARY $\mu$

Finite density QCD is symmetric under reflection of  $\mu$ ,  $Z(\mu) = Z(-\mu)$ , for both real and imaginary  $\mu$ . For imaginary  $\mu = i\mu_I$  it is moreover periodic,  $Z(\mu_I) = Z(\mu_I + 2\pi/3)$  [7]. Hence, certain shifts in  $\mu_I$  are equivalent to  $Z(3)$  transformations to different vacua. Consequently,  $Z(3)$  transitions occur at the critical values  $(\mu/T)^c = (k + 1/2)2\pi/3$ . The  $Z(3)$  sectors can be identified by monitoring the phase of the Polyakov loop. Ref. [7] predicts these transitions to be of first or-

\*Talk given by O. P.

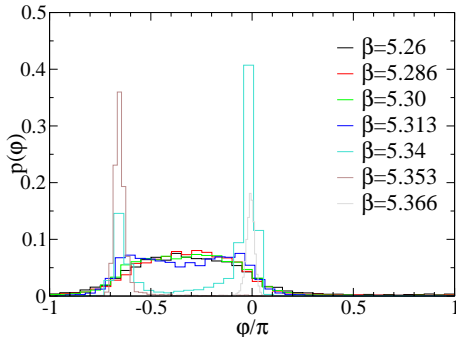


Figure 2. Probability distribution of the phase of the Polyakov loop for the critical value  $a\mu_I^c = \pi/12$ .

der for  $T > T_c$  and crossover for  $T < T_c$ , with the critical deconfinement temperature  $T_c$ . Schematically, the phase diagram is shown in Fig. 1, which is periodically repeated for larger  $\mu_I$ .

Our simulations support this picture. Fig. 2 shows the phase of the Polyakov loop at  $(\mu/T)^c$  for various lattice couplings/temperatures. A smooth distribution is found for low temperatures, whereas at high temperatures the two-state distribution signals a first order phase transition. Similar findings are reported for four flavors in [8]. The existence of a Z(3) transition with its endpoint joining on the deconfinement transition implies that the critical line of the latter becomes non-analytic at that point, and hence only  $\mu_I \leq \pi/3$  can be continued to real  $\mu$ .

Note that the deconfinement line as well as all observables even under reflections  $\mu \rightarrow -\mu$  are symmetric around the Z(3) transition. This is a feature that is not reproduced by reweighting from a Monte Carlo ensemble generated at  $\mu = 0$ , since such an ensemble does not sufficiently probe the other Z(3) sectors [6,2].

### 3. CONTINUATION OF THE DECONFINEMENT LINE

One method to locate a phase transition is to look for the peak  $\chi_{max} = \chi(\mu_c, \beta_c)$  of the susceptibilities  $\chi = VN_t \langle (\mathcal{O} - \langle \mathcal{O} \rangle)^2 \rangle$ , where we have used the plaquette, the chiral condensate and the Polyakov loop as operators  $\mathcal{O}(x)$ . Since simulations are always performed on finite volumes, sus-

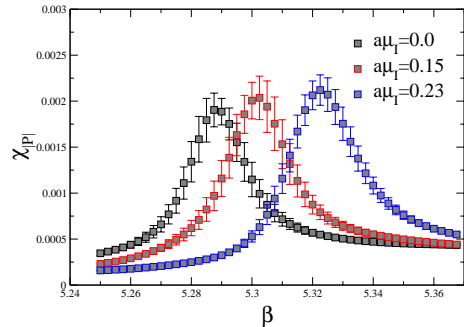


Figure 3. Susceptibilities of the modulus of the Polyakov loop for various  $\mu_I$ .

ceptibilities are analytic functions over the whole parameter space of the theory. Non-analyticities associated with phase transitions develop only in the thermodynamic limit.

For a given finite volume, the pseudo-critical line is then found by locating  $\chi_{max}$  for every  $\mu$ ,

$$\left. \frac{\partial \chi}{\partial \beta} \right|_{\beta_c} = 0 \quad \left. \frac{\partial^2 \chi}{\partial \beta^2} \right|_{\beta_c} < 0. \quad (1)$$

This is an implicit definition of the critical coupling  $\beta_c(\mu)$ . For analytic  $\chi(\mu, \beta)$  the implicit function theorem implies that also  $\beta_c(\mu)$  is analytic for all  $\mu$ . Moreover, the symmetry considerations of the last section ensure  $\beta_c(\mu) = \beta_c(-\mu)$ , so that we can expand in  $\mu/T = aN_t\mu$  to obtain

$$\beta_c(\mu) = \sum_n c_n (a\mu)^{2n}. \quad (2)$$

As long as, for imaginary  $\mu = i\mu_I$ , the non-perturbative data are well described by a few coefficients in this series, analytic continuation to real  $\mu$  simply proceeds by the operation  $\mu_I \rightarrow i\mu_I$ . This provides us with the location of the pseudo-critical line on a finite volume.

If there is a first order deconfinement transition ending in a critical point, then, as the volume is increased,  $\beta_c(\mu)$  approaches the line of phase transitions, while remaining pseudo-critical in a crossover regime. In principle, the nature of the line can be determined from the way the thermodynamic limit is approached,  $(\beta_c(V) - \beta_c(\infty)) \sim V^{-\sigma}$ , with  $\sigma = 1$  or  $0 < \sigma < 1$  for a first or second order transition, respectively, and  $\sigma = 0$  for

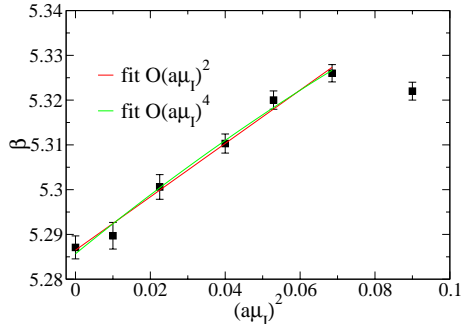


Figure 4. Location of the pseudo-critical deconfinement line as determined from plaquette susceptibilities. The lines show fits of the form Eq. 2 to quadratic and quartic order.

a crossover. Our first simulations are on a single volume and this question is postponed to future work.

Fig.3 shows a sequence of susceptibilities for the modulus of the Polyakov loop, with similar pictures for the plaquette and the chiral condensate. All three observables give statistically compatible values  $\beta_c(\mu_I)$ . Note that the peak is moving to larger  $\beta_c$  for growing  $\mu_I$ , as one would expect for imaginary  $\mu$ , cf. Eq. 2 and Fig. 1.

Fig. 4 shows  $\beta_c$  for different values of  $\mu_I$ . The data perfectly reproduce the expected symmetry of the partition function about the first  $Z(3)$  transition point. The lines in the figure show fits of a quadratic and a quartic polynomial to the data, with  $\chi^2/\text{dof} \approx 0.6$  and  $0.7$ , respectively. The coefficient of the quartic term is found to be zero within errors, and hence the two fits are statistically compatible: up to  $\mu_I/T = \pi/3$ , and for the quark flavors and masses under consideration, the critical line is well described by the quadratic term only.

After analytic continuation the result is transformed into physical units by means of the perturbative two-loop expression for the scale parameter  $a\Lambda_L$  and using  $T_c(\mu = 0)$  from the literature [9] to set the physical scale. We thus arrive at the phase diagram of Fig. 5, with the pseudo-critical line given by  $(\mu_B = 3\mu)$

$$\frac{T_c(\mu_B)}{T_c(\mu_B = 0)} = 1 - 0.00563(38) \left(\frac{\mu_B}{T}\right)^2. \quad (3)$$

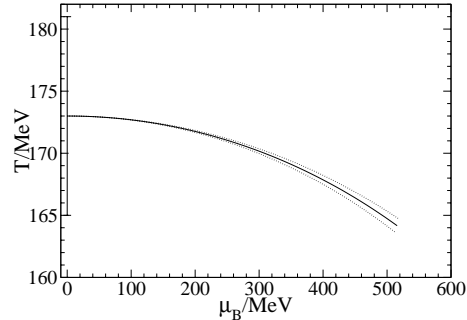


Figure 5. Location of the deconfinement transition. The error bar gives the uncertainty in  $T_c(0)$  used to set the scale, the dotted lines reflect the error on  $c_1$ , Eq. 2.

This result is consistent with those obtained by the reweighting approaches [2,3], for which it provides a crucial, controlled check. An important task ahead is to perform a finite size scaling analysis of the continued critical line, in order to determine the order of the transition as well as to locate a possible critical point.

## REFERENCES

1. For reviews and refs. see, e.g., S. Hands, Nucl. Phys. Proc. Suppl. **106** (2002) 142. O. Philipsen, Nucl. Phys. Proc. Suppl. **94** (2001) 49.
2. Z. Fodor and S. D. Katz, JHEP **0203** (2002) 014; Phys. Lett. B **534** (2002) 87.
3. C. R. Allton *et al.*, hep-lat/0204010.
4. M. P. Lombardo, Nucl. Phys. Proc. Suppl. **83** (2000) 375.
5. A. Hart, M. Laine and O. Philipsen, Phys. Lett. B **505** (2001) 141. Nucl. Phys. B **586** (2000) 443.
6. P. de Forcrand and O. Philipsen, hep-lat/0205016, to appear in Nucl. Phys. B.
7. A. Roberge and N. Weiss, Nucl. Phys. B **275** (1986) 734.
8. M. D'Elia and M. P. Lombardo, hep-lat/0205022.
9. F. Karsch, E. Laermann and A. Peikert, Nucl. Phys. B **605** (2001) 579.